Collective flow and particle spectra in relativistic heavy ion collisions

Heng Liu [a] for the E895 Collaboration [b]:
N.N. Ajitanand, J. Alexander, D. Best†, F.P. Brady, T. Case, W. Caskey, D.A. Cebra, J. Chance, P. Chung, B. Cole, K. Crowe, A. Das, J. Draper, M. Gilkes, S. Gushue, M. Heffner, A.S. Hirsch, E. Hjort, L. Huo, M. Justice, M. Kaplan, D. Keane, D. Krofcheck, R. Lacey, H. Liu, Y.M. Liu, M. Lisa, R. McGrath, Z. Milosevich, G. Odyniec, D.L. Olson, C. Pinkenburg, N. Porile, G. Rai, H.G. Ritter, J. Romero, R. Scharenberg, B. Srivastava, L. Schroeder, N.T.B. Stone, T.J.M. Symons, S. Wang, J. Whitfield, T. Wienold†, L. Wood, X. Yang, W.N. Zhang, Y. Zhang

[a]Physics Department, Kent State University, Kent, OH 44242, USA

[b]LBNL-UC Davis-Kent State-Ohio State-SUNYSB–Purdue-CMU-BNL-Columbia-Harbin Inst. of Tech.,China-Auckland,New Zealand

The E895 experiment has undertaken a systematic and exclusive study of Au+Au collisions between 2-8A GeV. Complete event-by-event data were obtained using the EOS time projection chamber (TPC) which provided good particle identification and continuous tracking over almost 4π solid angle. In central Au+Au collisions at 6A GeV, the proton rapidity distribution indicates almost complete stopping, hence high baryon density. We present preliminary results on collective flow observables as a function of beam energy. Data are compared with theoretical predictions.

1. Introduction

At AGS energies, collisions of heavy ions provide a unique opportunity for studying nuclear matter far from its normal density. It was predicted that at energy density about 1.5 GeV/fm^3 (10 times that of the nuclear ground state), a new form of matter Quark-Gluon Plasma (QGP) may be formed [1,2]. One promising way to search for the QGP is to measure the systematics of QGP signatures as a function of beam energy. By varying the beam energy from 2-10A GeV, one probes regions of temperature and baryon density where new and interesting phenomena are predicted to occur [3–6]. For example, directed flow could be sensitive to the pressure generated in a collision. Observing a sudden pressure change might suggest a deconfinement transition. From very low energies up through CERN SPS energies, measurements of fragment spectra from central Au/Pb + Au/Pb collisions indicate a pattern of steadily increasing freeze-out temperatures and expansion speeds up to at least 1A GeV [7], while a saturation of both these observables is apparent above 10A GeV or so [8–11]. Thus, E895 data span the potentially important region of transition between these two distinct types of behavior.

† Alexander von Humboldt Foundation (Lynen) Fellow

In this paper, a short description of the E895 experiment is presented followed by preliminary results from E895 and a physics discussion. The data used for these analyses represent a subset of the available statistics and are without final calibrations.

2. The Experiment E895

The E895 experiment investigates the global characteristics of nuclear matter at high energy and baryon density, with a specific emphasis on the energy dependence of collective observables. During January 1996 and November 1996, high statistics Au beam data were recorded at four beam energies: 2, 4, 6 and 8A GeV. The main E895 detector system is the EOS TPC [12], located inside the MPS magnet operated with a field of 0.75 or 1 T. The TPC provides continuous tracking, nearly 4π acceptance, and particle identification via energy loss measurement.

The TPC is constructed in the shape of a rectangular box and made up of an active drift volume with 154 cm in the beam direction, 96 cm wide in the bending direction and 75 cm high in the drift direction. The TPC tracks charged particles of $Z < 8$ by measuring the ionization loss and the time taken for this ionization to reach the bottom pad plane of the TPC. The pad plane is segmented into 128 rows and 120 columns of pads. Each pad samples 140 time buckets (100ns each) along the drift direction, therefore providing a complete 3 dimensional event readout.

3. Results and Discussion

3.1. Transverse mass spectra

Figure 1 presents preliminary transverse mass distributions for protons and negative charged pions, which have been measured over a wide range of rapidities for Au+Au collisions at 6A GeV. These data are for the most central 15% of geometric cross section.

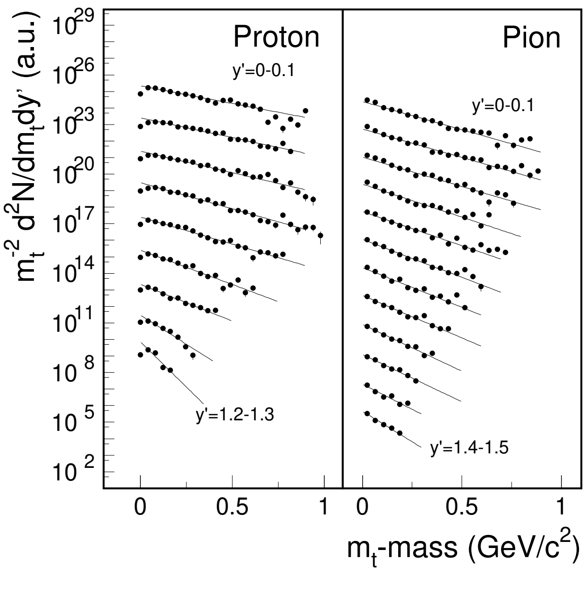

Figure 1. Preliminary E895 transverse mass spectra for protons and pions. The data are presented in normalized rapidity bins of 0.1 units. Successive spectra are scaled up by a factor of 10. Only statistical error bars are shown.

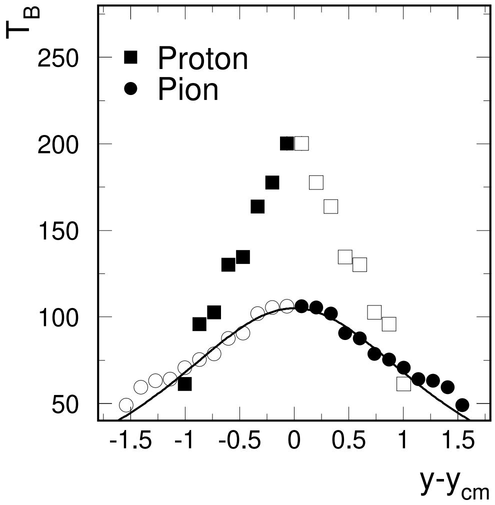

Figure 2. Inverse slope constants as a function of rapidity. The closed symbols are direct measurements and the open symbols are generated by reflection about midrapidity.

One of the key features of the TPC is that its acceptance extends down to $p_t = 0$. The spectra are plotted on a log scale and the Boltzmann-like distributions are represented by straight lines. At forward rapidity, the range of transverse mass $m_t = \sqrt{p_t^2 + mass^2}$ becomes smaller due to the phase space constraints.

Generally, the thermal distribution provides a reasonable description of the data for both protons and pions in a given rapidity window. Some statistically significant detail in Figure 1 is barely visible because of the large symbol size in relation to the vertical scale. For pions, a clear excess production over the thermal distribution is observed at low p_t. This could be explained by the contribution from baryon decays, mainly the Δ resonances [13]. For the proton data, the transverse mass distributions have a "shoulder-arm" shape which deviates from a purely thermalized fireball spectrum. This is typical characteristic of collective expansion for massive particles in heavy-ion collisions [14,7,9].

In Figure 2, we summarize the extracted slope parameters of protons (squares) and pions (circles) as a function of rapidity. The solid line is the calculation from a purely thermal model,

$$T_B = \frac{T_0}{\cosh(y - y_{cm})} \tag{1}$$

with $T_0 = 110$ MeV.

The experimental slope parameter measures the total particle energy comprising thermal and collective contributions. Assuming a common expansion velocity, collective energy is proportional to particle mass whereas thermal energy is independent of mass [15]. This is reflected in the prominent difference between the proton and pion spectra at mid-rapidity. It has been shown [9] that a common freeze-out temperature combined with a common expansion velocity can account for the difference in spectra between different particles.

The purely thermal fit works well for pions. This is easily understandable, since they are expected to thermalize easily due to their light mass and large interaction cross section in nuclear matter. Furthermore, pion spectra are not as affected as those of heavier particles by a given collective flow velocity and thus are reasonable probes for studying thermal properties at freeze-out.

3.2. Nuclear stopping

Because a substantial part of the populated phase space is measured in E895, this experiment is well suited for addressing nuclear stopping. Nucleon rapidity distributions yield information on nuclear stopping, which in turn provides a measure of how much initial participant kinetic energy is deposited into the excited system during the collision [16].

The proton rapidity distribution shown in Figure 3 is obtained by integrating the transverse mass spectra where data are available and extrapolating to $p_t = \infty$ using the Boltzmann fits. The open symbols are obtained by reflecting the experimental results about y_{cm}. The structure near the beam rapidity originates from spectators.

We can see from the data that a large fraction of protons are piled up at midrapidity, indicating a considerable amount of stopping, and therefore high baryon density, has been achieved at this energy.

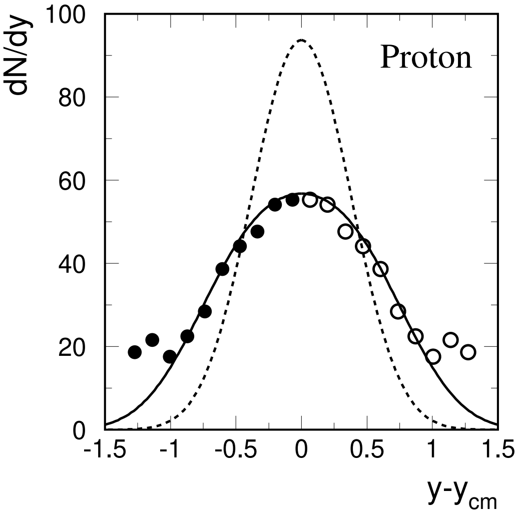

Figure 3. Proton rapidity distribution for Au+Au collisions at 6A GeV. The closed symbols are direct measurements and the open symbols are generated by reflection about midrapidity. The solid line represents a longitudinally expanding fireball, an isotropic thermal fireball calculation is shown as the dashed line.

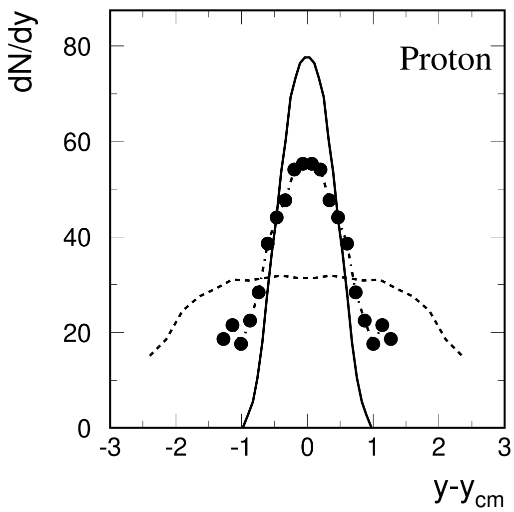

Figure 4. Proton rapidity distributions from 158A GeV Pb+Pb [18] (dashed line), 1.15A GeV Au+Au (solid line) and 6A GeV Au+Au (solid circles) collisions.

In Figure 3, an isotropic thermal model distribution with $T = 0.11$ GeV is shown as the dashed line. The observed rapidity distribution is wider than the simple thermal model. On the other hand, the calculation for a longitudinally expanding fireball [17] (solid line) using the same temperature and including an average expansion velocity of $\beta_z = 0.4c$ best describes the data. In this physical picture local isotropic sources are equally distributed over a rapidity interval centered at midrapidity.

The proton rapidity distributions for 158A GeV Pb+Pb (dashed line) [18], 1.15A GeV Au+Au (solid line) and 6A GeV Au+Au (solid circles) collisions are shown in Figure 4.

The Bevalac data are close to a single fireball distribution, while the SPS data are more extended in rapidity space.

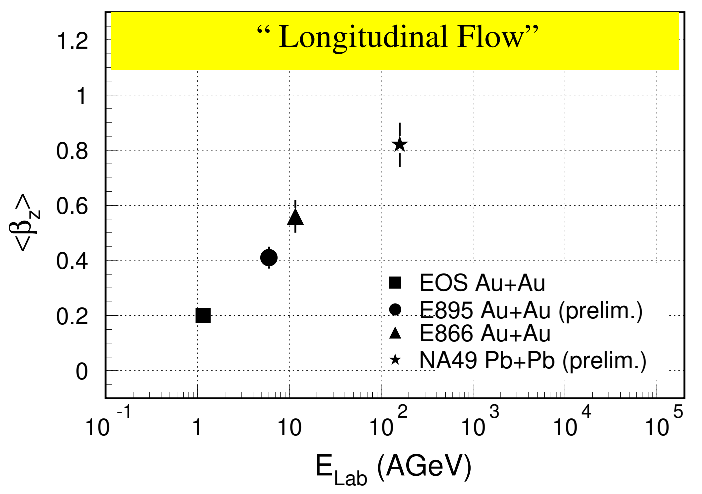

Figure 5. The dependence of the average longitudinal expansion velocity on beam energy.

The dependence of the average longitudinal expansion velocity on beam energy is shown in Figure 5. Note that the centrality cut is slightly different for the different experiments. Clearly, the higher the collision energy, the larger the value of the longitudinal flow velocity parameter. However, this picture cannot distinguish between expansion after complete stopping as opposed to transparency of two incident nuclei.

3.3. Directed Flow

Detection of a majority of the charged particles in the TPC allows us to study the average p_t correlation with the reaction plane directly. The global transverse momentum analysis of Danielewicz and Odyniec [19] has been performed to study the directed flow.

The impact parameter of the collision is infered from the measured charged baryon multiplicity. The data are divided into multiplicity bins in a manner similar to the Plastic Ball analysis [20]. For intermediate impact parameter collisions (Mult 4) where the flow signals are largest, Figure 6 shows the mean transverse momentum for free and bound protons projected onto the reaction plane as a function of the normalized rapidity $y' = (y_{lab} - y_{cm})/(y_{beam} - y_{cm})$. A typical "S"-shaped curve is observed. The estimated reaction plane dispersion angle is about 55°.

The Relativistic Quantum Molecular Dynamics (RQMD) model (version 2.3) [21] running in cascade mode (dashed line) underpredicts the $\langle p_x \rangle$ data. The inclusion of the mean field potential (solid line) increases the directed flow and leads to better agreement with the data.

The aim of the directed flow studies is to ultimately gain insight into the equation of state of hot and compressed matter. In an ideal relativistic one-fluid hydrodynamic model, Rischke [4] has calculated the directed flow as a function of beam energy, with and without a deconfinement phase transition. A phase transition leads to a very characteristic beam energy dependence of the flow signal due to the softening of the equation of state. Of course, the position of the minimum along the E_{lab} axis and its depth are quite sensitive to

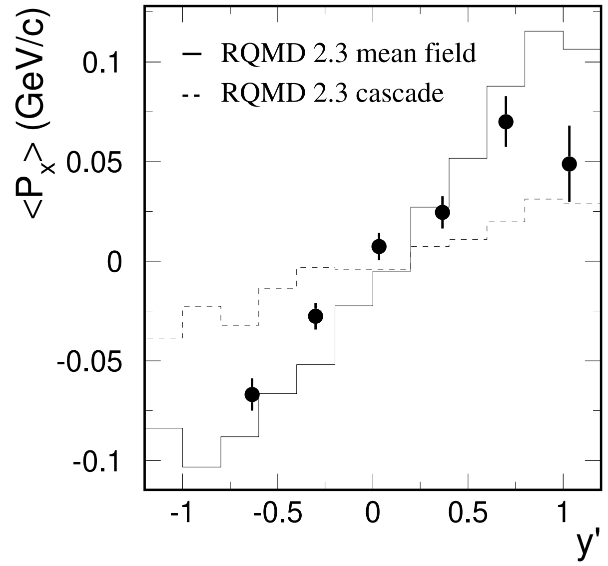

Figure 6. $< P_x >$ vs normalized rapidity y'. The data are from events in multiplicity bin 4 (see text).

details of the model calculation; nevertheless, such calculations are a good illustration of the general principle that an excitation function spanning the beam energy region where a mixed phase first appears may offer the best hope of observing evidence of QGP.

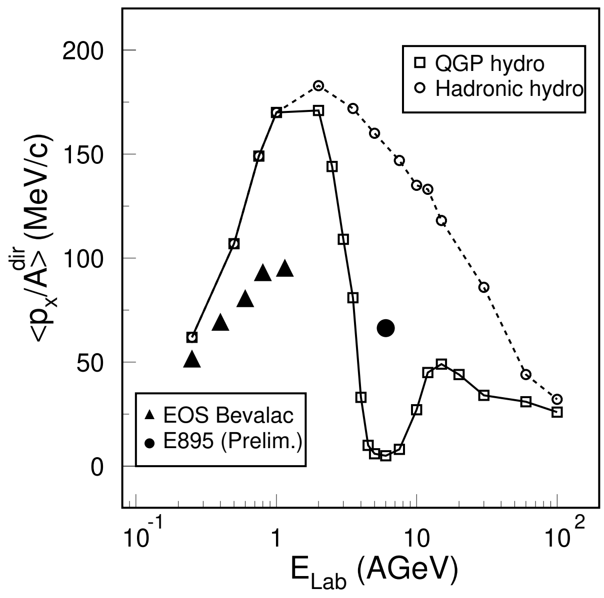

Figure 7. Directed flow as a function of beam energy. The EOS/Bevalac data are shown as solid triangles and the E895 point for $6A$ GeV is a solid circle.

In Figure 7 we show the hydrodynamic prediction along with the Bevalac data from EOS (solid triangles) and the point from E895 at $6A$ GeV (solid circle). Hydrodynamic calculations in general tend to overpredict the magnitude of directed flow, and so the comparison with data in Figure 7 should be focused only on the shape of the excitation functions. At this stage of our preliminary analysis, we conclude only that the directed flow, as characterized by Rischke's observable $\langle p_x/A\rangle^{\rm dir}$ [4], appears to have dropped significantly between the highest Bevalac energies and $6A$ GeV. The shape of the $\langle p_x \rangle$ excitation function is still under investigation, and data points at 2, 4 and $8A$ GeV will become available soon.

4. Summary

We have presented preliminary data on particle distributions and collective flow of hadrons produced in Au+Au collisions at $6A$ GeV using the 4π detector EOS TPC. The rapidity distribution at $6A$ GeV indicates a high degree of stopping. Fitting the data with a longitudinally expanding fireball model, we infer that the average expansion velocity increases smoothly with the logarithm of the beam energy. The inverse slope parameters depend on the particle mass and the pions are good probe for studying thermal properties at freeze-out. The freeze-out temperature at $6A$ GeV is about 110 MeV. The RQMD cascade calculation underpredicts the observed sideward flow and the mean-field prediction is closer to the data. The directed flow is lower than that at maximum Bevalac energy ($1A$ GeV for Au+Au collisions).

5. Acknowledgements

The author wishes to express his thanks to the organizers of this conference for the opportunity to present the first results on flow from E895, and to N. Xu for many helpful discussions and constant support.

REFERENCES

1. T.D. Lee and G.C. Wick, Phys. Rev. **D9**, 2291(1974).
2. F. Karsch, Nucl. Phys. **A590** 367c(1995).
3. C.M. Hung and E.V. Shuryak, Phys. Rev. Lett. **75**, 4003(1995)
4. D.H. Rischke, Nucl. Phys. **A610** 88c(1996).
5. H. Sorge, Phys. Rev. Lett. **78**, 2309(1997).
6. L.A. Winckelmann *et al.*, Nucl. Phys. **A610** 116c(1996).
7. M.A. Lisa *et al.*, EOS Collaboration, Phys. Rev. Lett. **75**, 2662(1995)
8. N. Xu *et al.*, NA44 collaboration, Nucl. Phys. **A610** 175c(1996).
9. I.G. Bearden *et al.*, NA44 Collaboration, Phys. Rev. Lett. **78**, 2080(1997)
10. T. Abbott *et al.*, Phys. Rev. **C50**, 1024(1994).
11. Z. Chen, Int. J. Mod. Phys. **E2**, 285(1993).
12. G. Rai *et al.*, IEEE Trans. Nucl. Sci. **37**, 56(1990).
13. J. Barrette *et al.*, E814 Collaboration, Phys. Lett. **B351**, 93(1995).
14. P.J. Siemens and J.O. Rasmussen, Phys. Rev. Lett. **42**, 880(1979)
15. K. Lee, U. Heinz, and E. Schnedermann, Z. Physik **C48** 525(1990).
16. M. Gyulassy, Nucl. Phys. **A590**, 431c(1995).
17. N. Xu (E814 collaboration), Proceedings of the 10th Winter Workshop on Nuclear Dynamics, (World Scientific, Singapore, 1994).
18. M. Toy, LBNL NSD annual report (1996).
19. P. Danielewicz and G. Odyniec, Phys. Lett. **157B**, 146(1985).
20. H.A. Gustafsson *et al.*, Phys. Rev. Lett. **52**, 1590(1984).
21. H. Sorge, Phys. Rev. **C52** 3291(1995).